Process Biochemistry 134 (2023) 32–43

Contents lists available at ScienceDirect

Process Biochemistry

journal homepage: www.elsevier.com/locate/procbio

Investigation of cellular and molecular mechanisms of caffeic acid phenethyl ester loaded nanoparticle systems in breast cancer cell lines

Fatma Sayan Poyraz [a], Reyhan Dilsu Colpan [a], Serap Derman [b], Banu Mansuroglu [a], Aysegul Erdemir [a,*]

[a] Department of Molecular Biology and Genetics, Faculty of Arts & Science, Yildiz Technical University, Istanbul, Turkey
[b] Department of Bioengineering, Faculty of Chemical and Metallurgical Engineering, Yildiz Technical University, Istanbul, Turkey

ARTICLE INFO

Keywords:
CAPE
Polymeric nanoparticle
Breast cancer
Anti-tumor activity

ABSTRACT

Breast cancer is associated with high morbidity and mortality in women since conventional treatment methods are limited due to toxicity problems and inadequate targeting of cancer cells. The aim of this study is to develop caffeic acid phenethyl ester (CAPE) loaded polymeric nanoparticles to provide treatment for breast cancer and investigate their anti-tumor activity on MCF-7 and MDA-MB-231 breast cancer cells. CAPE was encapsulated into poly lactic-co-glycolic acid (PLGA) polymer using single-emulsion (o/w) solvent evaporation method and characterization of CAPE loaded PLGA nanoparticles (CAPE-NPs) were performed by particle size, zeta potential, polydispersity index, in vitro release profile, and surface morphology. CAPE-NPs were tested for cytotoxicity, anti-migration, anti-proliferation and apoptotic activities on breast cancer cells. The mean nanoparticle size was found as 196,1 ± 8982 nm and polydispersity index (PDI) was 0186 ± 0069. The results of the in vitro cell culture studies indicated that treatment of breast cancer cells with CAPE and CAPE-NPs inhibited cell viability and proliferation. IC_{50} values for 48 h were determined as 28.35 μg/ml,19.57 μg/ml for CAPE and CAPE-NP, respectively. Additionally, CAPE-NPs induced intrinsic pathway of apoptosis in MCF-7 and MDA-MB-231 cell lines. Overall, CAPE-NPs showed more efficient anti-tumour activity on breast cancer cells by small size and enhanced bioavability.

1. Introduction

Breast cancer is one of the malignant tumors causing high mortality in women [1] and it's categorized into three different subtypes as hormone receptor-positive / HER-2 negative, hormone receptor-negative / HER-2 positive, and triple-negative [2]. Breast cancer, as a heterogeneous disease, has different risk profiles depending on distinct subtypes [3]. Hormone receptor positive/ HER-2 negative is the most common subtype among patients [4] while triple-negative tumors which distinguished by the lack of ER, PR an HER-2 genes are tend to be highly aggressive and recurrent [5].

Different treatment methods including endocrine therapy, chemotherapy, radiotherapy, and surgery are applied for different subtypes of breast cancer [6]. Therapy strategies are usually determined according to tumor subtype and cancer stage. Specific anti-HER-2 antibodies including trastuzumab and pertuzumab and tyrosine kinase inhibitors such as lapatinib and neratinib can be used for treatment of HER-2 positive breast cancers [7]. However, endocrine therapy is effective for hormone receptor positive patients whereas triple negative breast cancer is resistant to endocrine therapy [2]. In addition, conventional methods used in breast cancer treatment have low outcomes due to severe side effects, drug resistance, and low bioavailability of anti-cancer drugs [8]. Therefore, alternative therapeutic strategies are needed to eliminate disadvantages of traditional methods.

There has been an increased interest to nutritional therapies for several cancer types including breast cancer [9]. Bioactive molecules which isolated from food products can be used for cancer treatment due to extensive range of activities such as anti-cancer, anti-neoplastic and pharmaceutical [10]. CAPE is one of the bioactive compounds of propolis extract and presents anti-cancer, anti-oxidant, anti-inflammatory, anti-microbial and anti-viral activities [11]. CAPE has been shown to induce survival and growth, angiogenesis and apoptosis mechanisms in various cancers including breast cancer [12]. Previous in vitro and in vivo studies showed that CAPE inhibits ER+ PR+ (MCF-7 cells) and

Abbreviation: CAPE, (Caffeic Acid Phenethyl Ester); NP, (Nanoparticle); CAPE-NPs, (CAPE-loaded-Nanoparticles); PLGA, (Poly Lactic-co-Glycolic Acid).

* Corresponding author.
E-mail address: aerdemir@yildiz.edu.tr (A. Erdemir).

https://doi.org/10.1016/j.procbio.2023.09.016
Received 6 January 2023; Received in revised form 11 August 2023; Accepted 14 September 2023
Available online 15 September 2023
1359-5113/© 2023 Elsevier Ltd. All rights reserved.

triple negative (MDA-MB-231 cells) breast cancer cells growth via inducing cell cycle arrest and apoptosis [13]. Although CAPE exhibits several advantageous properties for breast cancer treatment, it has some disadvantages such as low bioavailability, low stability, and poor solubility [14]. Thus pharmaceutical use of CAPE in breast cancer treatment is limited.

Nanoparticle systems have become a powerful strategy for cancer diagnosis and treatment in terms of enabling controlled drug release and improving drug potency [15]. Particularly, polymeric nanoparticle studies have received attention due to promising future for cancer therapy in recent years. PLGA, as a synthetic polymer, have been used widely to produce polymeric nanoparticles to enhance controlled release, biodegradability, and biocompatibility of drugs [16].

In this study, we aimed to develop CAPE loaded nanoparticles for an enhanced anti-tumor activity on breast cancer cells. For this aim, we developed CAPE loaded PLGA nanoparticles and extensively investigated the in vitro anti-cancer activity on MCF-7 and MDA-MB-231 breast cancer cells.

2. Materials and methods

2.1. Reagents, materials and kits

CAPE, PLGA (lactide:glycolide=50:50), and polyvinyl alcohol were purchased from Sigma Aldrich. Solvents, dichloromethane (DCM) and ethanol were obtained from Merck. Human breast cancer cell lines MDA-MB-231 (invasive), MCF-7 (non-invasive) and MCF-10A were procured from the American Type Culture Collection (ATCC, Manassas, VA). Direct-zol™ RNA MiniPrep kit (Zymo Research, R2050), SensiFAST™ cDNA Synthesis Kit (65054) and SensiFAST™ SYBR Lo-Rox (94020) kits were obtained from Bioline Reagents Ltd. Proliferating cell nuclear antibody (PCNA) (MS-106-P) was acquired from Thermo Scientific™. Apoptag Plus Peroxidase In Situ Apoptosis Detection Kit (Cat. No. S7101) was used to detect apoptosis with Terminal deoxynucleotidyl transferase dUTP nick end labeling (TUNEL). Anti-caspase-3 (ab13847) and anti-cleaved caspase-9 (ab2324) were purchased from Abcam and β-Actin antibody (4967 S) was purchased from Cell Signaling Technologies.

2.2. Synthesis of CAPE loaded PLGA nanoparticles

CAPE loaded nanoparticles were prepared by a single emulsion (o/w) solvent evaporation method [17]. 40 mg of CAPE and 100 mg PLGA were dissolved in ethyl alcohol and DCM, respectively and they were mixed. The obtained organic phase was added into 3% PVA and the mixture was probe sonicated (80 W) in an ice bath for 90 s (Bandelin Sonopuls, Germany). Then, the mixture was injected into 35 ml of 0.1% PVA solution under stirring conditions. Stirring was continued for 4 h at 700 rpm at room temperature to allow to the removal organic solvent. After 4 h, solution was centrifuged at 9000 rpm at 4 °C and rewashed three times with distilled water after centrifugation in order to remove PVA and free CAPE. Finally, nanoparticles were freeze dried and stored at − 20 °C for further experiments.

2.3. Characterization studies of polymeric nanoparticles

2.3.1. Analysis of mean particle size (Z-Ave), zeta potential (ζ), polydispersity index (PDI) and surface morphology

Mean particle size, zeta potential and polydispersity index of the polymeric nanoparticles were determined using the Zetasizer Nano ZS (Malvern Instruments, UK) and measurements were performed in triplicate. The surface morphology of the nanoparticles was investigated through atomic force microscopy (AFM). AFM (Shimadzu SPM 9600, Japan) studies were performed in a dynamic mode in 2-dimensional (2-D) and 3- dimensional (3-D) for the morphological examination of nanoparticles. 5 μl nanoparticle solution were dropped to freshly cleaved mica surface and incubated for 5 min. Mica surface was rinsed with distilled water and dried for 20 min and the analysis was performed.

2.3.2. Fourier-transform infrared (FT-IR) spectroscopy

Fourier-transform infrared (FT-IR) spectroscopy was allowed to present functional groups of free CAPE and nanoparticle formulation. The spectral range of free CAPE and CAPE-NPs were obtained from 650 cm^{-1} to 4000 cm^{-1} with resolution of 4 cm^{-1}. Air was used as a background of the FT-IR spectrum.

2.3.3. Reaction yield (RY), encapsulation efficiency (EE) and drug loading (DL)

Reaction yield, encapsulation efficiency and drug loading percentages of produced nanoparticles were calculated. The amount of encapsulation efficiency was determined by an indirect method that allowed the use supernatants after centrifugation of nanoparticles. The amount of CAPE in supernatant was detected via UV-Vis spectroscopy at 323 nm. Finally, following equations for reaction yield, encapsulation efficiency and drug loading were applied:

$$RY \quad (\%) = \frac{Amount \quad of \quad nanoparticles \quad produced}{Initial \quad amount \quad of \quad PLGA \quad and \quad CAPE} \times 100$$

$$EE \quad (\%) = \frac{Amount \quad of \quad CAPE \quad encapsulated \quad in \quad PLGA \quad nanoparticles \quad (mg)}{Initial \quad amount \quad of \quad CAPE \quad (mg)} \times 100$$

$$DL \quad (\%) = \frac{Amount \quad of \quad CAPE \quad encapsulated \quad in \quad PLGA \quad nanoparticles}{Amount \quad of \quad weighed \quad nanoparticles} \times 100$$

2.4. In Vitro drug release

In vitro drug release profile of CAPE loaded nanoparticles were investigated in PBS solution (pH 7.4). 5 mg of the nanoparticles were dissolved in 10 ml PBS and stirred at 200 rpm, 37 °C. At specific time points, 1 ml of release medium were taken and centrifuged at 9000 rpm for 20 min and replaced with fresh PBS (1 ml). Release concentration of CAPE was determined by UV spectrophotometer at 323 nm. Analysis of in vitro drug release was followed for 30-day period.

2.5. Cell culture

MCF-10A cells were cultured in MEGM Mammary Epithelial Cell Growth Medium BulletKit (Lonza CC-3150) while MDA-MB-231 and MCF-7 cells were passaged in Dulbecco's modified Eagle's medium (DMEM) (Sigma 6046)/Ham's Nutrient Mixture F-12 medium (1:1) (Gibco 21765–029), supplemented with 10% fetal bovine serum (FBS) (Gibco), streptomycin (100 μg/ml), penicilin (100 U/ml) and L-glutamine (0.2 mM). The cells were cultured in a humidified incubator containing 5% CO_2 at 37 °C.

2.6. In vitro cell viability assay

The effect of CAPE and CAPE loaded nanoparticles on cell viability was investigated on MCF-10A, MCF-7 and MDA-MB-231 cell lines using 3-[4,5-dimethylthiazol-2-yl]− 2,5 diphenyl tetrazolium bromide (MTT) assay. Briefly, the cells were grown in a 96 well plate at a seeding density of 1×10^4 per well. After overnight incubation, the cells were treated with free CAPE and CAPE-NPs at different concentrations and incubated for 24 and 48 h. Then, culture medium was discarded and 50 μl of MTT solution was added to each well and plates were incubated for 3 h until

developing formazan crystals. Subsequently, 100 μl of DMSO was added to dissolve formazan products and the absorbance was recorded on a microplate reader at 570 nm. The percentage of cell viability was calculated based on the following formula:

$$Cell\ \ viability\% = \frac{OD\ \ value\ \ of\ \ treated\ \ cells}{OD\ \ value\ \ of\ \ control\ \ cells} x100$$

2.7. Determination of cell proliferation

Proliferating cell nuclear antigen (PCNA) immunocytochemical method was employed to determine changes in cell proliferation. MDA-MB-231 and MCF-7 cells were seeded 1×10^4 cells/well on coverslip in a 24-well culture plate. Next day, cells were treated with free CAPE and CAPE-NPs at IC_{50} values and incubated 24 and 48 h. Then, cells were washed with phosphate-buffered saline (PBS) after removing complete culture medium and fixed using ice methanol for 5 min. Subsequently, blocking solution was added each well and PCNA primer antibody which was diluted at 1:300 ratio was applied on the cells for overnight at 4 °C. To detect of PCNA antibody, biotinylated secondary antibodies and streptavidin, biotinylated horseradish peroxidase (Invitrogen, USA) were used. Cells were revealed according to AEC kit (Invitrogen, USA) manufacturer's protocol. PCNA positive and negative cells were countered selecting 10 areas randomly. Finally, the percentage of proliferation was analyzed as follows:

$$PCNA\ \ positive\ \ cells\% = \left(\frac{total\ \ number\ \ of\ \ PCNA\ \ positive\ \ cells}{total\ \ cell\ \ number}\right) x100$$

2.8. TUNEL assay

Detection of apoptosis was conducted by TUNEL kit (S7101) according to manufacturer's protocol. In brief, MCF-7 and MDA-MB-231 cells were cultured at a density of 1×10^4 cells per well on coverslips in 24-well plates and treated with free CAPE and CAPE-NPs according to IC_{50} values. After 24 and 48 h incubation time, cells were fixed via methanol and equilibration buffer was added on the coverslips and waited 2 min. Then, reaction buffer and TdT enzyme were mixed and 50 μl of the mixture was added on the cells and incubated for 1 h at 37 °C. Stop wash was applied on the cells and washed with PBS at three times. Subsequently, anti-digoxigenin peroxidase was added and waited 30 min at room temperature. TUNEL-positive and negative cells were observed using diaminobenzidine (DAB) and hematoxylene-eosin staining. The percentage of apoptotic cells was calculated by counting 10 different random areas according to given formula:

$$TUNEL\ \ positive\ \ cells\% = \left(\frac{total\ \ number\ \ of\ \ TUNEL\ \ positive\ \ cells}{total\ \ cell\ \ number}\right) x100$$

2.9. Quantitative real-time polymerase chain reaction analysis

For quantitative real-time polymerase chain reaction (RT-qPCR) analysis, free CAPE and CAPE-NPs depending on IC_{50} values were applied on breast cancer cells. RNA isolation was carried out using Direct-zol™ RNA MiniPrep kit protocol and isolated RNA was transformed into cDNA using SensiFAST cDNA synthesis kit according to manufacturer's instructions. AriaMx Real-Time PCR System (USA) with SensiFAST SYBR Lo-Rox was used for RT-qPCR analysis. The PCR cycling conditions were set up at 95℃ for 5 s, 63℃ for 10 s and 72℃ for 15 s, 40 cycles after initial denaturation at 95℃ for 2 min. Primer pair sequences used in this study were listed on Table 1 and B-actin was used as an internal reference. Comparative CT method (ΔΔCt) was used to calculate relative gene expression for each gene [18].

2.10. Western blot analysis

Western blot analyses were performed as reported previously [19]. Cells were treated with free CAPE and CAPE-NPs at their IC_{50} concentrations and incubated for 24 and 48 h. Total protein was isolated from MCF-7 and MDA-MB-231 cells using 1x RIPA buffer and a protease inhibitor cocktail (Sigma PPC1010) mixture. Proteins were quantified with BCA Protein Assay kit (SMART™) manufacturer's protocol and equal amount of protein samples were separated by 4–12% sodium dodecyl sulfate polyacrylamide gel electrophoresis (SDS-PAGE). Trans-Blot® Turbo transfer system (Bio-Rad, USA) was used in order to transfer proteins onto PVDF membranes. Then, membranes blocked with non-fat powdered milk were incubated overnight at 4℃ with cytochrome-c (1:1000), caspase-3 (1:250), cleaved caspase-9 (1:500) and b-actin (1:1000) primary antibodies. After incubation time, membranes were washed with PBS-T for thrice. Subsequently, horseradish peroxidase-conjugated secondary antibodies (mouse-ab205719, rabbit-ab205718, 1:10000) were applied on membranes and incubated for 1 h at room temperature. After washing membranes with PBS-T, PBS and distilled water respectively, 3,3' diaminobenzidine (DAB) and H_2O_2 mixture were used to detect protein bands.

2.11. Statistical analysis

Statistical data were analysed using GraphPad Prism software version 6 (GraphPad Software, La Jolla, CA). Data were expressed as mean ± standard deviation (SD) and comparison of groups analysed using unpaired t-test. $p < 0.05$ were considered as statistically significant.

3. Results and discussion

3.1. Nanoparticle characterization

Studies on nanoparticle systems have significantly increased in

Table 1
Primer sequences used in this study for RT-qPCR.

Gene	Forward Primer	Reverse Primer
B-actin	5'-CATGTACGTTGCTATCCAGGC-3'	5'-CTCCTTAATGTCACGCACGAT-3'
Cytochrome-c NM_018947	5'-CTTTGGGCGGAAGACAGGTC-3'	5'-TTATTGGCGGCTGTGTAAGAG-3'
Caspase-3 NM_004346	5'-AGAGGGGATCGTTGTAGAAGTC-3'	5'-ACAGTCCAGTTCTGTACCACG-3'
Caspase-9 NM_032996	5'-CTCAGACCAGAGATTCGCAAAC-3'	5'-GCATTTCCCCTCAAACTCTCAA-3'
Caspase-8 NM_033356	5'-GTTGTGTGGGGTAATGACAATCT-3'	5'-TCAAAGGTCGTGGTCAAAGCC-3'
Bax NM_138763	5'-CCCGAGAGGTCTTTTTCCGAG-3'	5'-CCAGCCCATGATGGTTCTGAT-3'
Bcl-2 NM_000657	5'-GGTGGGGTCATGTGTGTGG-3'	5'-CGGTTCAGGTACTCAGTCATCC-3'

recent years, and these systems find applications across several domains. In particular, polymeric nanoparticles, formulated using biodegradable polymers, have garnered substantial attention due to their small sizes and bioavailability, demonstrating remarkable potential for treating diverse diseases and enabling targeted drug delivery [20]. Notably, PLGA nanoparticles offer exceptional utility within drug delivery systems for compounds with limited water solubility. Thus, this study involved the production of CAPE-loaded PLGA nanoparticles using the single emulsion solvent evaporation method. The objective was to address the unfavorable attributes of the CAPE molecule, known for its anti-cancer properties, by incorporating it into nanoparticle systems. This approach aimed to enhance water solubility and biocompatibility while evaluating the anti-cancer efficacy of the resultant CAPE-loaded nanoparticles against human breast cancer cell lines. The outcomes of the nanoparticle synthesis align with the CAPE-loaded nanoparticle systems previously discussed by Derman in the literature [21].

Characterization studies of the synthesized nanoparticles encompassed measurements of particle size, zeta potential, and polydispersity index, along with AFM, FT-IR, and in vitro release assessments. The Zeta Sizer (Malvern Zetasizer Nano ZS 90) was employed to conduct particle size distribution and zeta potential measurements for the CAPE-NPs. The average particle size of the nanoparticles was determined to be 196.1 ± 8.982 nm (Fig. 1A), with the mean zeta potential registering at − 21.97 ± 1.45 mV (Fig. 1B), and a polydispersity index of 0.186 ± 0.069. Encapsulation efficiency (EE) was calculated at 90.04%, retention yield (RY) at 41.83%, and drug loading (DL) at 61.52%.

FT-IR spectra of PLGA, free CAPE, and CAPE-NPs were analyzed to ascertain active substance-polymer interactions and to identify the presence of the active substance within or on the produced nanoparticles. Fig. 1C presents the FT-IR spectrum of PLGA polymer, free CAPE, and CAPE-NPs. Upon examining the FT-IR spectrum of the PLGA polymer, distinctive peaks associated with C-H stretching of C-H and CH2 at 2993 and 2989 cm-1, respectively, were observed. Notably, the sharp and robust peak around 1750 cm-1 corresponds to the C = O peak in the ester bond, while the range of 1160–1090 cm-1 represents the C-O bond tension band [17]. Conversely, the CAPE molecule displayed peaks at 3471 cm-1, 1332 cm-1, and 1600 cm-1. A comparison between the CAPE nanoparticle and PLGA spectra reveals the absence of CAPE-specific peaks, and the PLGA spectrum remains unaltered. Consequently, successful CAPE loading into the nanoparticles without surface adsorption is evident.

The release behavior of nanoparticles holds paramount importance for their application, directly influencing drug stability, therapeutic outcomes, and formulation development [22]. Release experiments for CAPE-NPs suspended in PBS buffer (pH: 7.4) were conducted under horizontal shaking at 200 rpm and 37 °C over a 30-day period. At the end of this duration, the CAPE-NPs released 46.77%, as depicted in Fig. 1D. In analyzing the in vitro release graph, a pattern similar to that observed by Villaverde emerges, indicating that the majority of the release occurs within the initial 3 h on average. This phenomenon is attributed to the "Burst effect," a rapid-release mechanism explained in the literature. This effect stems from the fraction of the drug in proximity to or loosely bound to the polymer nanoparticle surface, rather than the drug embedded within the nanoparticle matrix [23]. Following this initial effect, a slower and more controlled release ensues.

The nanoparticle's size significantly impacts its capacity to navigate the bloodstream and reach tumor tissue. Men et al. highlighted that small-sized nanoparticle systems can interact with tumor cells, facilitating passive tumor targeting through the enhanced permeability and retention (EPR) effect [24]. Small nanoparticles can accumulate and traverse tumor blood vessels efficiently, unlike larger nanoparticles that face barriers in vessel traversal and reaching the intended tumor tissue. Therefore, optimizing nanoparticle size generally aims to enhance tumor tissue-specific uptake [25]. Utilizing AFM, we explored the shape and surface morphology of CAPE-NPs. AFM images revealed that the produced CAPE-loaded nanoparticles possessed a spherical morphology and uniform size distribution, with average particle sizes consistent with those determined through dynamic light scattering, approximately ranging between 150 and 220 nm. These outcomes parallel those of esculetin-loaded PLGA nanoparticles developed by Kacar et al. [26].

3.2. Cell culture studies

3.2.1. Cytotoxic effect of CAPE and CAPE-NPs on MCF10A, MCF-7 and MDA-MB-231 cells

Nanoencapsulation of single or multiple bioactive compounds is currently widely used to enhance the anticancer activities of compounds against various cancer types [27]. It is well-known that CAPE exhibits anticancer activity across different types of cancer, including breast cancer. Another crucial attribute of CAPE is its lack of harm to healthy cells [13]. Therefore, to verify the safety of CAPE-NPs on healthy cells, cytotoxicity evaluation was initially performed on MCF10A mammary epithelial cells.

Fig. 2A and B depict the cytotoxic activity of CAPE and CAPE-NP on MCF10A cells for 24 and 48 h, respectively. Across all tested concentrations, neither CAPE nor CAPE-NP exhibited cytotoxic effects on MCF10A cells, confirming their safety for use.

Moreover, we investigated how CAPE-NPs influence cell viability in comparison with free CAPE in MCF-7 and MDA-MB-231 cells. Fig. 2C and Fig. 2D illustrate changes in MCF-7 cell viability after treatment with CAPE and CAPE-NP. The IC_{50} values for 24 h and 48 h were determined as 64.2 μg/ml and 28.35 μg/ml for CAPE, and 34.26 μg/ml and 19.57 μg/ml for CAPE-NP, respectively. As displayed in Fig. 2D, free CAPE also inhibited MCF-7 cell viability at higher concentrations such as 75 μg/ml and 100 μg/ml. Nevertheless, relative to the control and CAPE-NP treated groups, the most significant inhibition of MCF-7 cell viability was observed with CAPE-NP treatment for 48 h. CAPE-NP treatment exhibited increased cytotoxicity on the estrogen-positive (ER+) MCF-7 cell line in a dose and time-dependent manner.

Furthermore, we assessed the cytotoxic activity of CAPE and CAPE-NP on the triple-negative breast cancer cell line (TNBC), MDA-MB-231. TNBC, accounting for 10–15% of all breast cancer cases, poses a challenge due to the absence of any receptors on the cell surface [28]. Thus, finding effective strategies to prevent TNBC development is crucial. In vitro cytotoxicity evaluation of CAPE-NPs on MDA-MB-231 cells demonstrated a significant reduction in cell viability.

Both free CAPE molecules and CAPE-NPs were applied to the cells across a concentration range of 1–100 μg/ml, based on the in vitro drug release levels corresponding to 24th and 48th hour values. The graphs in Fig. 2 present cell viability rates corresponding to different concentrations of free CAPE and CAPE-NPs applied to the cells. IC50 values for both the free CAPE molecule and CAPE-NPs were determined based on the resulting graphs.

Fig. 2A and B illustrat% cell viability plots for MCF10A at 24 and 48 h, respectively. The cytotoxicity analysis conclusively revealed that the CAPE-loaded nanoparticle formulations had no cytotoxic impact on the MCF-10A cell line when compared to the free molecule.

Subsequently, we assessed the impact of CAPE-NPs on MCF-7 cell viability in comparison with the free CAPE molecule over 24 and 48 h. The calculated IC50 values were 64.2 μg/ml and 28.35 μg/ml for CAPE, and 34.26 μg/ml and 19.57 μg/ml for CAPE-NP, for 24 and 48 h, respectively. Percentage cell viability plots for the MCF-7 cell line are displayed in Figs. 2C and 2D.

Additionally, the effects of free CAPE and CAPE-NPs on cell viability in MDA-MB-231 breast cancer cells for 24 and 48 h are shown in Figs. 2E and 2F. As per the results, the IC50 value for free CAPE was determined as 21.75 μg/ml, and for CAPE-NPs, it was 15.50 μg/ml for 24 h (Fig. 2E). For the 48th hour, the IC50 values were 4.76 μg/ml for free CAPE and 4.75 μg/ml for CAPE-NPs (Fig. 2F).

The cytotoxic activity of both free CAPE and CAPE-NPs on MCF-7 and MDA-MB-231 cells highlighted the nanoparticle system's efficacy at lower doses in both cancer cell types compared to the free compound.

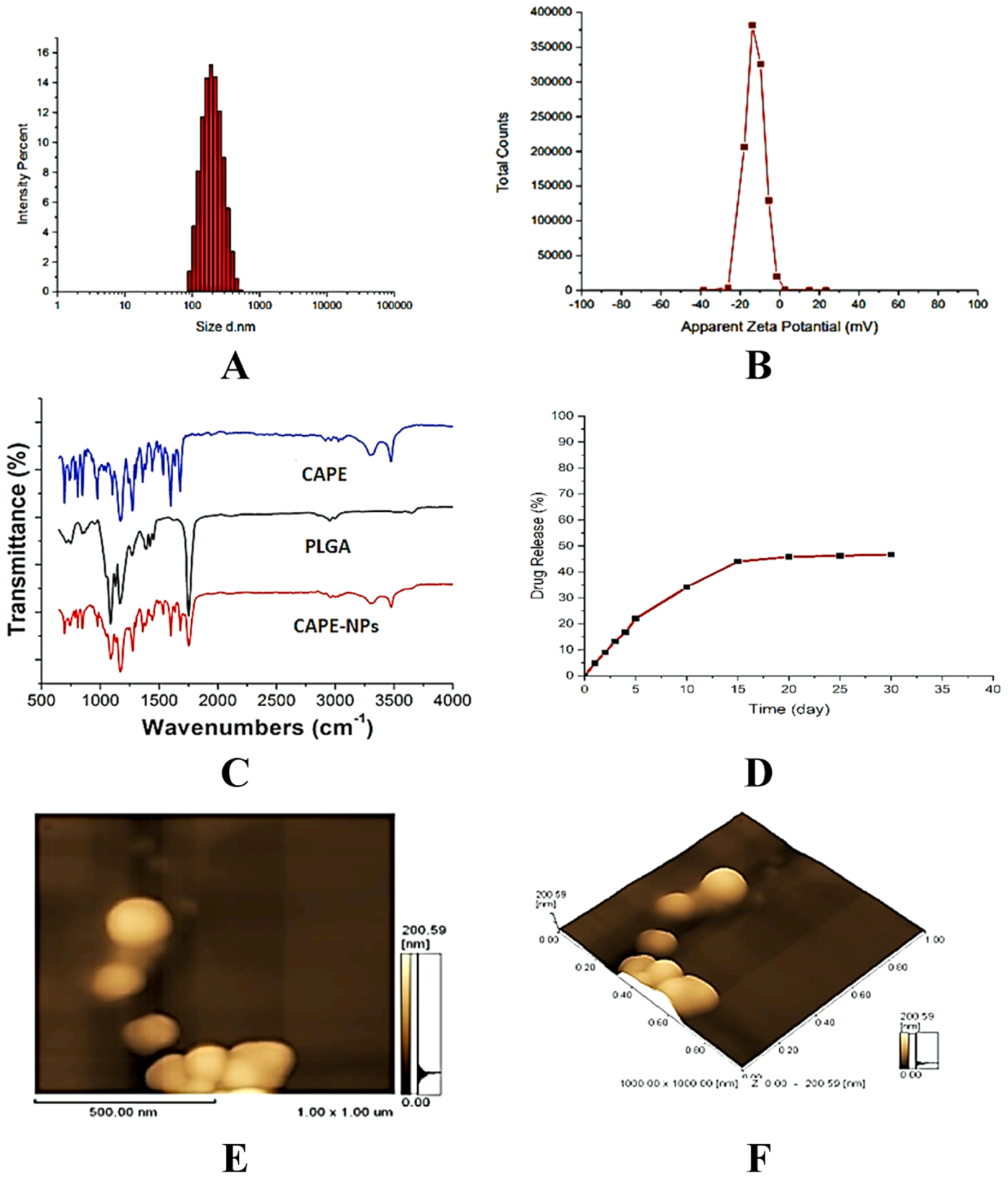


Fig. 1. Morphological and physicochemical characterization of caffeic acid phenethyl ester (CAPE) loaded poly lactic-co-glycolic acid (PLGA) nanoparticles (NPs). Dynamic light scattering (DLS) demonstrates the size distribution of CAPE-loaded PLGA nanoparticles (CAPE-NPs) (A). Zeta potential intensity distributions of CAPE-NPs (B). Fourier-transform infrared spectrums (FT-IR) of synthesized nanoparticles, PLGA polymer and free drug CAPE (C). In vitro drug release profile of CAPE-loaded poly lactic-co-glycolic acid nanoparticles (CAPE-NPs) in phosphate-buffered saline (PBS) at pH 7.4 (D). Representative 2D and 3D atomic force microscopy images of CAPE-loaded poly lactic-co-glycolic acid nanoparticles (CAPE-NPs) respectively (E-F).

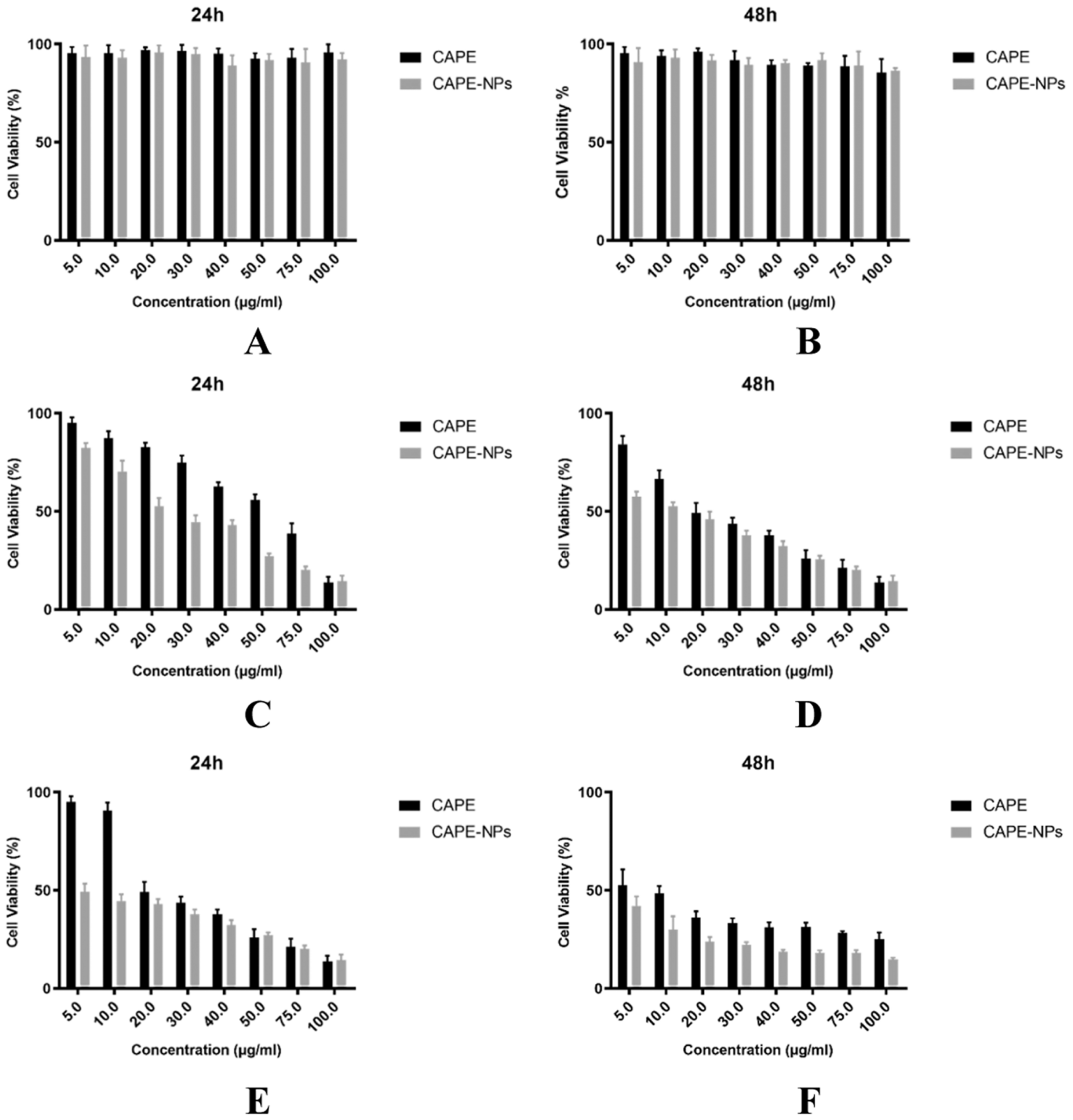


Fig. 2. Cytotoxicity analyses of caffeic acid phenethyl ester (CAPE) loaded poly lactic-co-glycolic acid (PLGA) nanoparticles (CAPE-NPs) in human breast cancer cells (MCF-7 and MDA-MB-231) and healthy human breast cells (MCF-10A). Dose and time-dependent cytotoxic activity of CAPE-NPs and free CAPE after 24 h (A) and 48 h (B) incubation with MCF-10A healthy breast cells. Dose and time-dependent cytotoxic activity of CAPE-loaded PLGA nanoparticles (CAPE-NPs) and free CAPE after 24 h (C) and 48 h (D) incubation with MCF-7 human breast cancer cells. Dose and time-dependent cytotoxic activity of CAPE-loaded PLGA nanoparticles (CAPE-NPs) and free drug CAPE after 24 h (E) and 48 h (F) incubation with MDA-MB-231 human breast cancer cells.

Furthermore, extended 48-hour incubation effectively suppressed the growth of breast cancer cells, particularly the MDA-MB-231 cell line. The encapsulation of CAPE within the PLGA polymer seemingly enhanced CAPE's solubility. This phenomenon parallels findings from Wang et al., where CAPE was encapsulated in skim milk microcapsules and its bioactivity against the HCT-116 colon cancer cell line was compared with free CAPE. The study demonstrated that due to the increased solubility and bioavailability of CAPE, the microcapsules exhibited enhanced antiproliferative activity against the HCT-116 cell line compared to free CAPE [29].

In another study, CAPE-loaded nanoparticles targeting mortalin, an abundant Hsp70 protein on the surface of cancer cells, were synthesized using anti-mortalin antibodies (MotAb) to enhance solubility. Targeted CAPE-MotAb exhibited enhanced anticancer activity in both in vitro and in vivo assays [30].

The literature distinctly portrays the high cytotoxic effects of

nanoparticle systems on various cancer cells by increasing drug solubility.

3.2.2. Anti-proliferative effect of free CAPE and CAPE-NPs on human breast cancer cell lines

The anti-proliferative effect of the CAPE molecule has been demonstrated in numerous cancer cell lines [31]. The impact of both free CAPE and CAPE-NPs on the proliferation of human breast cancer cells (MCF-7 and MDA-MB-231) was assessed through immunocytochemical PCNA labeling. The proliferation percentage of cells was determined by quantifying PCNA-labeled and non-labeled MCF-7 and MDA-MB-231 cells.

The proliferation percentage of both cell lines decreased following treatment with both free CAPE and CAPE-NPs, compared to the control cells. Incubating MCF-7 cells with free CAPE and CAPE-NPs for 24 h led to a 3% and 7% reduction in cell proliferation, respectively. Similarly, with a 48-hour incubation, free CAPE and CAPE-NPs resulted in a 1% and 8% inhibition of MCF-7 cell proliferation. Fig. 3 illustrates the anti-proliferative effects of free CAPE and CAPE nanoparticle formulations on MCF-7 cells.

Conversely, treating MDA-MB-231 cells with free CAPE and CAPE-NPs for 24 and 48 h led to a reduction of 3% and 17% for 24 h, and a decrease of 6% and 17% for 48 h in cell proliferation when compared to untreated cells. These results highlight that extended incubation with nanoparticles resulted in decreased cell division. Fig. 4 presents the anti-proliferative effects of free CAPE and CAPE-NPs applied to MDA-MB-231 cells.

The outcomes indicated that the synthesized CAPE-NPs exerted a more pronounced effect on the proliferation of human breast cancer cell lines MCF-7 and MDA-MB-231, in comparison to free molecules. In a study by Ersoz et al., it was demonstrated that loading hesperetin into the PLGA nanoparticle system increased its anti-proliferative activity against C6 glioma cancer cells [32]. Another study showcased the effective inhibition of cell proliferation through quercetin-loaded PLGA nanoparticles [33]. These findings collectively illustrate that nanoparticle systems facilitate the enhanced internalization of various drugs into cells, thereby reducing cell proliferation.

3.2.3. Apoptotic effect of free CAPE and CAPE-NPs on human breast cancer cell lines

Apoptosis, or programmed cell death, is associated with various diseases, including cancer, yet cancer cells often evade apoptosis [34]. The TUNEL assay is an in situ method used to detect apoptosis by visualizing nuclei containing fragmented DNA [35]. The Terminal deoxynucleotidyl transferase-mediated dUTP end labeling (TUNEL) kit was utilized to determine apoptotic cells following 24 and 48 h of treatment of breast cancer cells with CAPE and CAPE-NP.

After 24 h of incubation, the percentage of cells undergoing apoptosis was found to be 10% in MCF-7 control cells, 20% in MCF-7 cells treated with free CAPE, and 23% in MCF-7 cells treated with CAPE-NPs. Similarly, after 48 h of incubation, the apoptotic cell percentages were calculated as 11%, 28.74%, and 32.6% for the control, free CAPE, and CAPE-NPs, respectively. Fig. 5 illustrates the apoptotic activity of free CAPE and CAPE-NPs applied to MCF-7 cells. The highest apoptotic cell count, reaching 32.6%, was observed after treatment with CAPE-loaded nanoparticles, which are more potent inducers of apoptosis due to the controlled release of CAPE. Similarly, Ersoz et al. reported that hesperetin-loaded PLGA nanoparticles demonstrated enhanced apoptosis induction compared to free hesperetin in a glioma cell line [32]. Another study showed that encapsulated disulfiram molecules into PLGA exhibited higher apoptosis induction activity compared to the free drug on MCF-7 cells [36].

In the case of MDA-MB-231 cells, following 24-hour exposure to CAPE and CAPE-NPs, the ratio of cells undergoing apoptosis was approximately 8.97% in the control group, 15.11% for free CAPE, and 30% for cells treated with CAPE-NPs. Similarly, after 48 h of incubation, the apoptotic cell percentages were determined as 12.71%, 24.09%, and 41.44% for the control group, free CAPE, and CAPE-NPs, respectively. Fig. 6 presents the apoptotic effect on the MDA-MB-231 cell line. A study by Vijayan et al. demonstrated that paclitaxel-loaded nanoparticles induced apoptosis at a rate of 19.8% after 48 h in MDA-MB-231 cells [37].

Overall, the results for both cell lines indicate that cells treated with CAPE-NPs undergo a more pronounced apoptosis compared to cells treated with free CAPE. The nanoparticle formulation is believed to exert a more substantial impact on cells, driving them towards apoptosis due to its controlled release property, as opposed to the free molecule.

3.2.4. Determination of apoptotic effect of CAPE and CAPE nanoparticle by qPCR method

The real-time PCR method is among the most widely used techniques for determining gene expression, owing to its advantageous features such as a broad dynamic range, sensitivity, and not requiring post-amplification processing [38]. In this study, Real-Time PCR analysis was conducted on MCF-7 and MDA-MB-231 cells exposed to free CAPE and CAPE-NPs. Subsequently, the levels of cytochrome-c, caspase-3, caspase-9 (involved in the intrinsic apoptosis pathway), and caspase-8 (related to the extrinsic pathway) were quantified in comparison to the control group, along with B-actin gene expression. Similarly, the expression levels of the pro-apoptotic Bax and anti-apoptotic Bcl-2 were determined by comparison with the control group and B-actin gene expression.

Total RNA was extracted from MCF-7 and MDA-MB-231 cells treated with free CAPE and CAPE-NPs at the IC50 doses determined for 24 and 48 h. The purity of the isolated RNA samples was assessed, yielding A260/A280 ratios ranging from 2.04 to 2.21.

The isolated RNAs were then reverse transcribed into cDNA using the reverse transcriptase enzyme. Real-Time PCR was performed using the

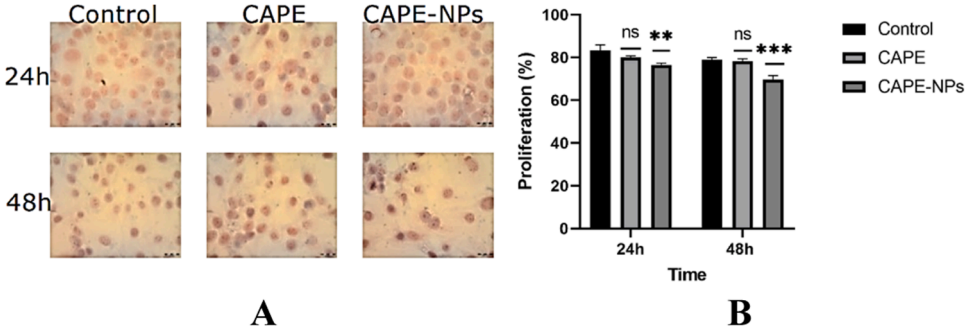


Fig. 3. The antiproliferative activity of free caffeic acid phenethyl ester (CAPE) and CAPE-loaded PLGA nanoparticles (CAPE-NPs) was determined on MCF-7 human breast cancer cells via proliferating cell nuclear antigen (PCNA) labelling. Quantification of PCNA-positive immunostained cells revealed CAPE-NPs had significantly decreased cell proliferation compared to control ($p < 0.05$) for 24 h and 48 h (B). The brightfield microscope images show PCNA-positive labelled MCF-7 cells (red) (A). The data were represented as means ± SD with $n = 3$ for each group.

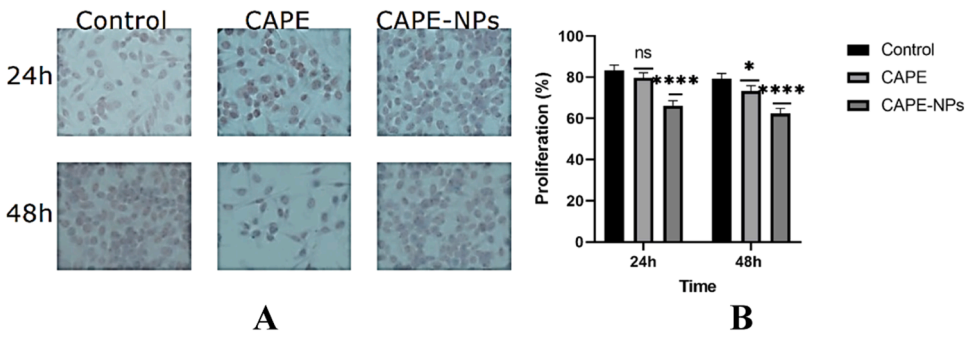


Fig. 4. The antiproliferative activity of free caffeic acid phenethyl ester (CAPE) and CAPE-loaded poly lactic-co-glycolic acid nanoparticles (CAPE-NPs) was determined on MDA-MB-231 human breast cancer cells via proliferating cell nuclear antigen (PCNA) labelling. Quantification of PCNA-positive immunostained cells revealed CAPE-NPs had significantly decreased cell proliferation compared to control ($p < 0.05$) for 24 h and 48 h. Compared to free CAPE, CAPE-NPs had significantly decreased cell proliferation for only 48 h ($p < 0.05$). It was insignificant for 24 h (B). The brightfield microscope images show PCNA-positive labelled MDA-MB-231 cells (red) (A). The data were represented as means ± SD with n = 3 for each group.

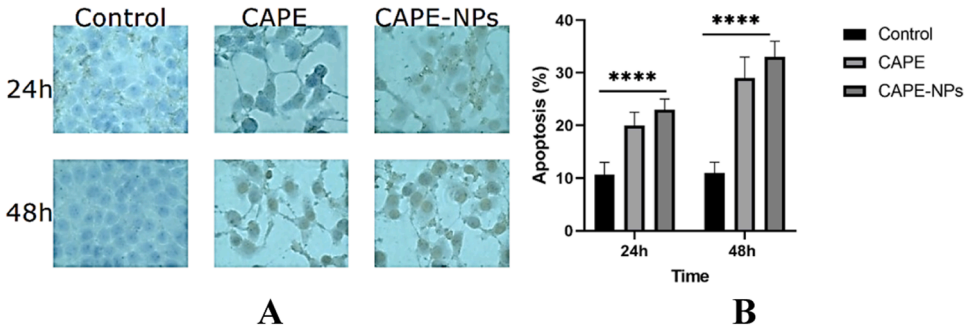


Fig. 5. The antiapoptotic activity of free caffeic acid phenethyl ester (CAPE) and CAPE-loaded poly lactic-co-glycolic acid nanoparticles (CAPE-NPs) was determined on MCF-7 human breast cancer cells via terminal deoxynucleotidyl transferase dUTP nick end labelling (TUNEL). Quantification of apoptotic cells revealed CAPE-NPs had significantly increased apoptosis in MCF-7 cells compared to control and free CAPE ($p < 0.01$) for 24 h and 48 h (B). The brightfield microscope images show apoptotic cells (brown) (A). The data were represented as means ± SD with n = 3 for each group.

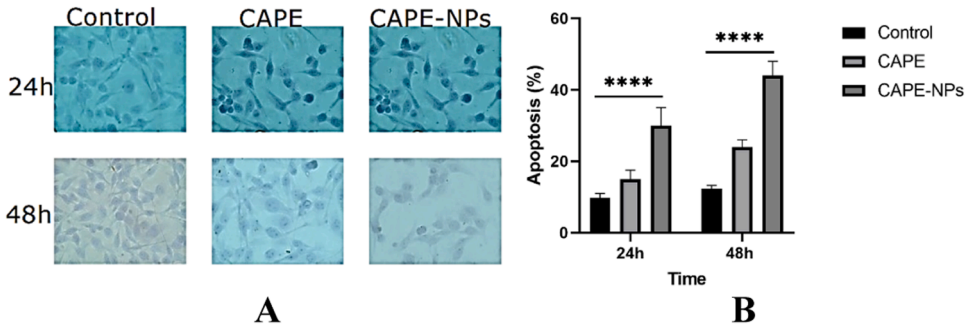


Fig. 6. The antiapoptotic activity of free caffeic acid phenethyl ester (CAPE) and CAPE-loaded poly lactic-co-glycolic acid nanoparticles (CAPE-NPs) was determined on MDA-MB-231 human breast cancer cells via terminal deoxynucleotidyl transferase dUTP nick end labelling (TUNEL). Quantification of apoptotic cells revealed CAPE-NPs had significantly increased apoptosis in MDA-MB-231 cells compared to control and free CAPE ($p < 0.01$) for 24 h and 48 h (B). The brightfield microscope images show apoptotic cells (brown) (A). The data were represented as means ± SD with n = 3 for each group.

diluted cDNAs (at a ratio of 1:4), forward and reverse primers for each gene, and SYBR green dye. The expression of target genes was analyzed using the 2-ΔΔt method, comparing it with B-actin gene expression in the gene group that remained unchanged under the conditions [18]. The relative mRNA expressions of caspase-3, caspase-9, cytochrome-c, Bcl-2, Bax, and caspase-8 genes relative to the control were presented in Fig. 7.

As a result of treating MCF-7 (Fig. 7A) and MDA-MB-231 (Fig. 7B) cells with free CAPE and CAPE-NPs for 24 h, Bcl-2 expression decreased by 0.08 and 0.07 times for free CAPE and CAPE-NPs in MCF-7 cells, respectively, and decreased by 0.078 and 0.082 times in MDA-MB-231 cells. Following intracellular apoptotic stimulation, Bid, a pro-apoptotic member, inactivates the anti-apoptotic protein Bcl-2 and activates Bax and Bak proteins [39]. Bax expression increased 2.48 and 2.53 times in MCF-7 cells for free CAPE and CAPE-NPs, and 3.12 and 3.23 times in MDA-MB-231 cells, respectively, illustrating the interplay between Bcl-2 and Bax. A similar observation was made by Montazeri et al., who reported comparable results after curcumin nano-formulation, showing changes in mRNA levels of apoptosis-related genes involving Bcl-2 and Bax in hepatocarcinoma cell lines [40]. However, after 48 h of treatment, Bax and Bcl-2 expressions remained similar in both free CAPE and CAPE nanoparticle-treated MCF-7 (Fig. 7C) and MDA-MB-231 (Fig. 7D) cells.

In MCF-7 cells, cytochrome-c, which is released from mitochondria, showed a 2.3-fold increase in expression after 48-hour treatment with

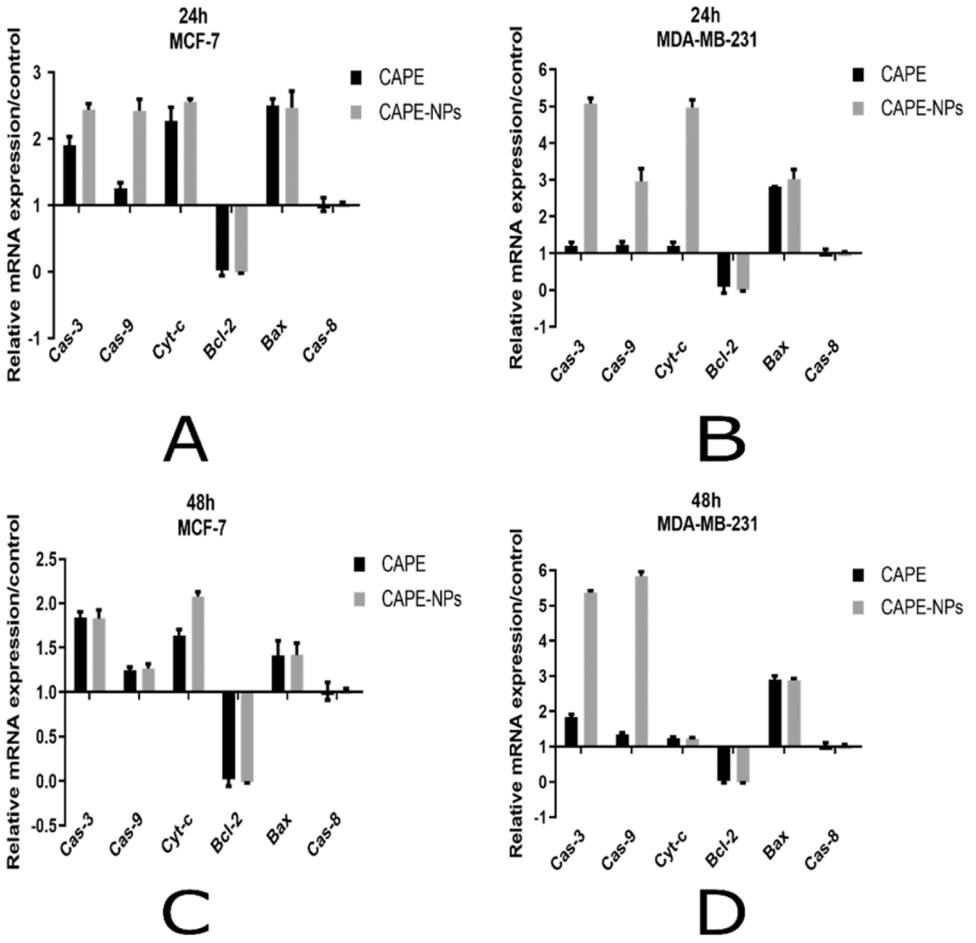


Fig. 7. Relative expressions of caspase-3 (Cas-3), caspase-9 (Cas-9), cytochrome-c (Cyt-c), Bcl-2, Bax, and caspase-8 (Cas-8) genes relative to control. Quantitative real-time PCR analysis of mRNA levels of apoptotic genes in caffeic acid phenethyl ester (CAPE) loaded poly lactic-co-glycolic acid nanoparticles (CAPE-NPs) treated human breast cancer cells MCF-7(A) and MDA-MB-231(B) on 24 h. Quantitative real-time PCR analysis of mRNA levels of apoptotic genes in CAPE-NP treated human breast cancer cells MCF-7(C) and MDA-MB-231(D) on 48 h.

the nanoparticle formulation, whereas this gene expression was 5 times higher than the control after 24-hour treatment in MDA-MB-231 cells. Furthermore, 48-hour application of CAPE nanoparticles increased caspase-9 expression in MDA-MB-231 cells by 5.21 times (Fig. 7D), while this gene expression remained nearly stable in MCF-7 cells (Fig. 7C) compared to the control. The activation of Caspase-3 by the Caspase-9 gene increased by almost 5.5-fold compared to the control. Conversely, Caspase-8 expression, pivotal in the extrinsic pathway, remained steady at the mRNA level in both cell lines. Abou-El-Naga et al. found that polymeric nanoparticles induced the intrinsic apoptosis pathway in breast cancer cells, resulting in 2.8-fold and 1.6-fold increases in the expression of caspase-9 and caspase-3 genes, respectively [41]. Similarly, a significant increase in caspase-3 expression was observed, around 4 and 2.5-fold, after treatment with 5-fluorouracil and curcumin loaded PLGA nanoparticles in the Hep-2 cell line [42]. In conclusion, by comparatively examining pro-apoptotic and anti-apoptotic genes, it was revealed that CAPE-NPs induce the intrinsic pathway of apoptosis.

3.2.5. Demonstration of apoptosis induction of CAPE and CAPE-NPs at protein levels

Apoptosis is characterized by morphological changes involving many biochemical processes, including activation of caspases. This process is controlled by the internal or external means. Cytochrome-c and caspase-9 are involved in the mitochondrial pathway, while caspase-3 is known to be a key mediator of apoptosis because it is involved in both pathways [34].

The demonstration of the apoptotic effect of free CAPE and CAPE-NPs on MCF-7 and MDA-MB-231 cells at the protein level was performed by Western Blot method. In the study, free CAPE and CAPE-NPs were applied on MCF-7 and MDA-MB-231 cells for 24 and 48 h, and the expression of cytochrome-c, caspase-3 and cleaved caspase-9 proteins, which are involved in the intrinsic pathway of apoptosis, were investigated.

After treatment of free CAPE and CAPE-NPs, protein expression levels were verified on cytochrome-C (12 kDa), caspase-3 (35 kDa) and cleaved-caspase-9 (37 kDa) in MCF-7 and MDA-MB-231 cells. The B-actin gene, which is in the reference gene group whose expression does not change according to the conditions, was used as a loading control (Fig. 8).

The results of expression of cytochrome-c illustrated that only CAPE nanoparticle treatment activated the cytochrome-c expression for 24- and 48-hour samples in both MCF-7 and MDA-MB-231 cells. In our study, it was found that the apoptotic effect exhibited by the CAPE nanoparticle formulation was similar to the apoptotic effect of PLGA nanoparticles loaded with chelidonine on HepG2 cells by Paul et al. [43]. As a result, nanoparticle formulation is thought to induce apoptosis in MCF-7 and MDA-MB-231 cell lines by stimulating the intrinsic pathway.

Caspase-9, which is among the frequently studied inducing caspases,

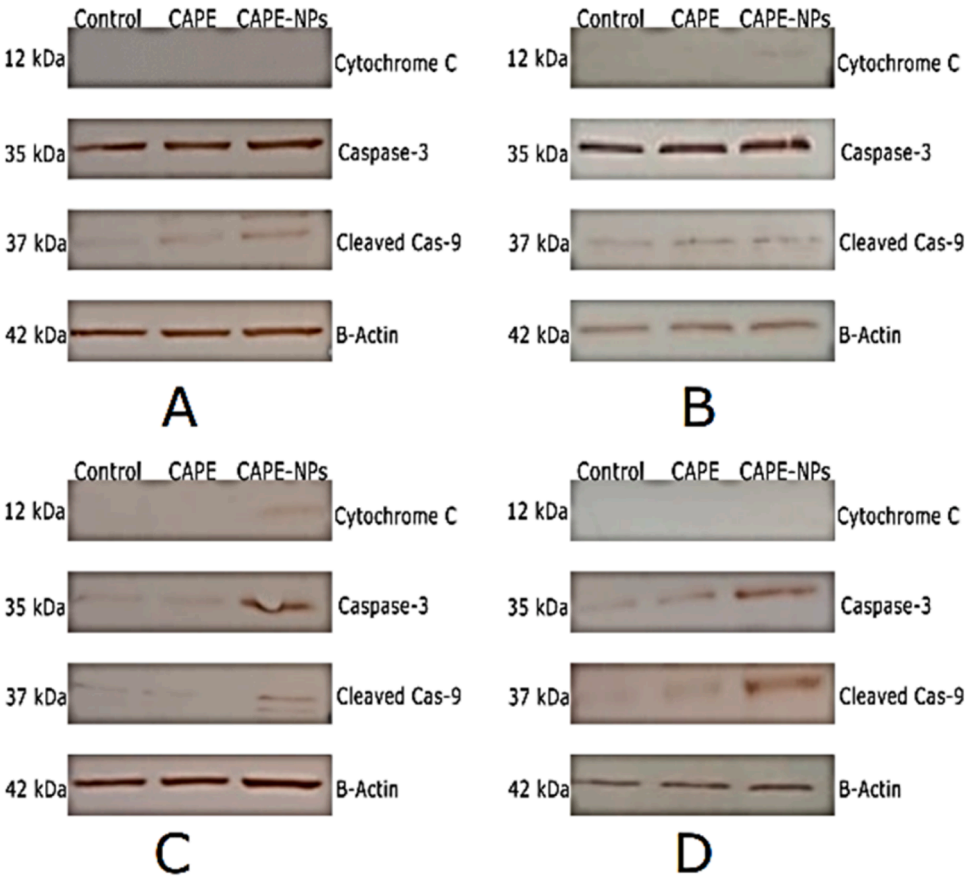


Fig. 8. Protein expression levels of cytochrome-c, cleaved-caspase-9, and caspase-3 proteins in CAPE loaded poly lactic-co-glycolic acid nanoparticles (CAPE-NPs) treated human breast cancer cells MCF-7 (A-24 h and B-48 h) and MDA-MB-231 (C-24 h and D-48 h) were analyzed by western blotting. β-actin was used as a loading control.

is an important protein in the intrinsic pathway of apoptosis against various stimuli such as chemotherapy, stress agents and radiation [44]. In apoptotic process, caspase-9 turns into cleaved form. Therefore, cleaved caspase-9 expression was examined after free CAPE and CAPE loaded nanoparticle treatment on MCF-7 cells and consequences of cleaved caspase-9 expression levels found to be higher on CAPE-NPs treated cells than free CAPE treated cells. On the other hand, the expression was high in MDA-MB-231 cells treated with CAPE-NPs. A significant expression was observed especially at 48th hour results compared to MCF-7 cells.

After free CAPE and CAPE-NPs treated on MCF-7 and MDA-MB-231 cells at 24 and 48 h; caspase-3 activation was observed in all samples. As a result of the Western Blot analysis of caspase-3 expression, increasing expression was observed in both samples in the control, CAPE and CAPE-NPs, respectively. A stronger expression was found in MCF-7 cells compared to MDA-MB-231 cells. It is thought that some cells in the control group show a low level of caspase-3 expression due to their tendency to apoptosis in the long incubation period. When the free CAPE and CAPE-NPs are compared, it is seen that caspase-3 shows a higher level of expression in the CAPE nanoparticle. These results showed that the nanoparticle formulation produced is more effective compared to the free molecule and provides caspase-3 activation by directing cells to apoptosis. Moreover, Mata et. al. produced gold nanoparticles for colon cancer and the results showed that induction of apoptosis occurred via caspase-9 and caspase-3 protein expression [45]. Another study demonstrated that curcumin loaded nanoparticles triggered the mitochondrial apoptotic pathway of human oral cancer cells through upregulating protein expression levels of cyt-c, caspase-3 and caspase-9 [46]. These studies in parallel with our study suggest that the nanoparticle formulation is more effective in directing cells to apoptosis than free molecule and activates the intrinsic pathway of apoptosis.

4. Conclusion

In summary, despite the multifaceted therapeutic potential of CAPE encompassing anti-tumor, anti-oxidant, anti-inflammatory, anti-microbial, and anti-viral activities, its practical utility has been limited by challenges like poor solubility, low bioavailability, and instability. This investigation sought to overcome these limitations by harnessing the capabilities of nanoparticle systems, leading to the successful encapsulation of the CAPE molecule within PLGA polymer using the single emulsion solvent evaporation technique.

The resultant CAPE-NPs exhibited a particle size of 196.1 ± 8.982 nm, a key feature that contributed to their heightened cytotoxicity compared to free CAPE. This augmented cytotoxicity can be attributed to their compact size and controlled release profile. Furthermore, CAPE-NPs demonstrated the capacity to curtail cell proliferation while provoking the intrinsic apoptotic pathway, effectively triggering the activation of cytochrome-c and caspases in breast cancer cells.

Our findings underscore the beneficial impact of encapsulating CAPE within PLGA polymer, yielding enhancements in bioavailability, release kinetics, cytotoxic efficacy, as well as anti-proliferative and anti-apoptotic effects by virtue of improved solubility. Nevertheless, while our study offers promising insights, further investigations are essential to assess the clinical viability of these findings.

In conclusion, this research sheds light on the potential of

nanoparticle-based delivery systems to augment the therapeutic properties of CAPE, bringing us closer to addressing its limitations and advancing its applicability in clinical settings.

Funding

This study was supported by Research Foundation of Yildiz Technical University under grant FBA-2018-3254.

Declaration of Competing Interest

The authors declare that they have no known competing financial interests or personal relationships that could have appeared to influence the work reported in this paper.

Data Availability

Data will be made available on request.

References

[1] L. Iacoviello, M. Bonaccio, G. de Gaetano, M.B. Donati, Epidemiology of breast cancer, a paradigm of the "common soil" hypothesis, in: In Seminars in Cancer Biology, 72, Academic Press, 2021, pp. 4–10, https://doi.org/10.1016/j.semcancer.2020.02.010.

[2] A.G. Waks, E.P. Winer, Breast cancer treatment: a review, Jama 321 (3) (2019) 288–300, https://doi.org/10.1001/jama.2018.19323.

[3] M.E. Barnard, C.E. Boeke, R.M. Tamimi, Established breast cancer risk factors and risk of intrinsic tumor subtypes, Biochim. Et. Biophys. Acta (BBA)-Rev. Cancer 1856 (1) (2015) 73–85, https://doi.org/10.1016/j.bbcan.2015.06.002.

[4] Y. Han, J. Wang, Z. Wang, B. Xu, Comparative efficacy and safety of CDK4/6 and PI3K/AKT/mTOR inhibitors in women with hormone receptor-positive, HER2-negative metastatic breast cancer: a systematic review and network meta-analysis, Curr. Probl. Cancer 44 (6) (2020) 100606–100623, https://doi.org/10.1016/j.currproblcancer.2020.100606.

[5] M. Ravi, S. Tentu, G. Baskar, S. Rohan Prasad, S. Raghavan, P. Jayaprakash, G. Venkatraman, Molecular mechanism of anti-cancer activity of phycocyanin in triple-negative breast cancer cells, BMC Cancer 15 (1) (2015) 13, https://doi.org/10.1186/s12885-015-1784-x.

[6] P.R. Dandawate, D. Subramaniam, R.A. Jensen, S. Anant, Targeting Cancer Stem Cells and Signaling Pathways by Phytochemicals: Novel Approach for Breast Cancer Therapy, in: In Seminars in Cancer Biology, 40, Acedemic Press, 2016, pp. 192–208, https://doi.org/10.1016/j.semcancer.2016.09.001.

[7] S. Escrivá-de-Romaní, M. Arumí, M. Bellet, C. Saura, HER2-positive breast cancer: current and new therapeutic strategies, Breast 39 (2018) 80–88, https://doi.org/10.1016/j.breast.2018.03.006.

[8] N. Olov, S. Bagheri-Khoulenjani, H. Mirzadeh, Combinational drug delivery using nanocarriers for breast cancer treatments: a review, J. Biomed. Mater. Res. Part A 106 (8) (2018) 2272–2283, https://doi.org/10.1002/jbm.a.36410.

[9] R. Venugopal, R.H. Liu, Phytochemicals in diets for breast cancer prevention: the importance of resveratrol and ursolic acid, Food Sci. Hum. Wellness 1 (2012) 1–13, https://doi.org/10.1016/j.fshw.2012.12.001.

[10] S. Esposito, A. Bianco, R. Russo, A. Di Maro, C. Isernia, P.V. Pedone, Therapeutic perspectives of molecules from Urtica dioica extracts for cancer treatment, Molecules 24 (2019) 2753–2776, https://doi.org/10.3390/molecules24152753.

[11] L. Cornara, M. Biagi, J. Xiao, B. Burlando, Therapeutic properties of bioactive compounds from different honeybee products, Front. Pharmacol. (2017), 412, https://doi.org/10.3389/fphar.2017.00412.

[12] C. Omene, M. Kalac, J. Wu, E. Marchi, K. Frenkel, O.A. O'Connor, Propolis and its active component, caffeic acid phenethyl ester (CAPE), modulate breast cancer therapeutic targets via an epigenetically mediated mechanism of action, J. Cancer Sci. Ther. 5 (10) (2013) 334–342, https://doi.org/10.4172/1948-5956.1000224.

[13] J. Wu, C. Omene, J. Karkoszka, M. Bosland, J. Eckard, C.B. Klein, K. Frenkel, Caffeic acid phenethyl ester (CAPE), derived from a honeybee product propolis, exhibits a diversity of anti-tumor effects in pre-clinical models of human breast cancer, Cancer Lett. 308 (1) (2011) 43–53, https://doi.org/10.1016/j.canlet.2011.04.012.

[14] R. Wadhwa, N. Nigam, P. Bhargava, J.K. Dhanjal, S. Goyal, A. Grover, S.C. Kaul, Molecular characterization and enhancement of anticancer activity of caffeic acid phenethyl ester by γ cyclodextrin, J. Cancer 7 (13) (2016) 1755–1771, https://doi.org/10.7150/jca.15170.

[15] K.H. Wong, A. Lu, X. Chen, Z. Yang, Natural ingredient-based polymeric nanoparticles for cancer treatment, Molecules 25 (16) (2020) 3620–3644, https://doi.org/10.3390/molecules25163620.

[16] M. Hashemi, A. Shamshiri, M. Saeedi, L. Tayebi, R. Yazdian-Robati, Aptamer-conjugated PLGA nanoparticles for delivery and imaging of cancer therapeutic drugs, Arch. Biochem. Biophys. 691 (2020) 108485–108496, https://doi.org/10.1016/j.abb.2020.108485.

[17] T. Arasoglu, S. Derman, B. Mansuroglu, Comparative evaluation of antibacterial activity of caffeic acid phenethyl ester and PLGA nanoparticle formulation by different methods, Nanotechnology 27 (2) (2015), 025103, https://doi.org/10.1088/0957-4484/27/2/025103.

[18] K.J. Livak, T.D. Schmittgen, Analysis of relative gene expression data using real-time quantitative PCR and the 2− ΔΔCT method, Methods 25 (4) (2001) 402–408, https://doi.org/10.1006/meth.2001.1262.

[19] R.D. Colpan, A. Erdemir, Co-delivery of quercetin and caffeic-acid phenethyl ester by polymeric nanoparticles for improved antitumor efficacy in colon cancer cells, J. Microencapsul. 38 (6) (2021) 381–393, https://doi.org/10.1080/02652048.2021.1948623.

[20] A. Zielińska, F. Carreiró, A.M. Oliveira, A. Neves, B. Pires, D.N. Venkatesh, E. B. Souto, Polymeric nanoparticles: production, characterization, toxicology and ecotoxicology, Molecules 25 (16) (2020) 3731–3751, https://doi.org/10.3390/molecules25163731.

[21] S. Derman, Caffeic acid phenethyl ester loaded PLGA nanoparticles: effect of various process parameters on reaction yield, encapsulation efficiency, and particle size, 318-318, J. Nanomater. 16 (1) (2016), https://doi.org/10.1155/2015/341848.

[22] X.Y. Lu, D.C. Wu, Z.J. Li, G.Q. Chen, Polymer nanoparticles, Prog. Mol. Biol. Transl. Sci. 104 (2011) 299–323, https://doi.org/10.1016/B978-0-12-416020-0.00007-3.

[23] A. Villaverde, Nanoparticles in Translational Science and Medicine, 104, Academic Press, 2011. ISBN: 9780124160200.

[24] K. Men, X. Duan, X. Wei Wei, M. Ling Gou, M. Juan Huang, L. Juan Chen, Y. Quan Wei, Nanoparticle-delivered quercetin for cancer therapy, Anti-Cancer Agents Med. Chem. (Former. Curr. Med. Chem. -Anti-Cancer Agents) 14 (6) (2014) 826–832, https://doi.org/10.2174/1871520614666140521122932.

[25] S. Tran, P.J. DeGiovanni, B. Piel, P. Rai, Cancer nanomedicine: a review of recent success in drug delivery, Clin. Transl. Med. 6 (2017) 1–21, https://doi.org/10.1186/s40169-017-0175-0.

[26] A. Karatug Kacar, F. Bahadori, S.E. Kepekci Tekkeli, G. Topcu, S. Bolkent, Investigation of cell death mechanism and activity of esculetin-loaded PLGA nanoparticles on insulinoma cells in vitro, J. Pharm. Pharmacol. 72 (4) (2020) 592–606, https://doi.org/10.1111/jphp.13228.

[27] L. Ma, M. Kohli, A. Smith, Nanoparticles for combination drug therapy, ACS Nano 7 (11) (2013) 9518–9525, https://doi.org/10.1021/nn405674m.

[28] N. Garmpis, C. Damaskos, A. Garmpi, K. Nikolettos, D. Dimitroulis, E. Diamantis, A. Nonni, Molecular classification and future therapeutic challenges of triple-negative breast cancer, vivo 34 (4) (2020) 1715–1727, https://doi.org/10.21873/invivo.11965.

[29] A. Wang, M. Leible, J. Lin, J. Weiss, Q. Zhong, Caffeic acid phenethyl ester loaded in skim milk microcapsules: Physicochemical properties and enhanced in vitro bioaccessibility and bioactivity against colon cancer cells, J. Agric. Food Chem. 68 (50) (2020) 14978–14987, https://doi.org/10.1021/acs.jafc.0c05143.

[30] J. Wang, P. Bhargava, Y. Yu, A.N. Sari, H. Zhang, N. Ishii, R. Wadhwa, Novel caffeic acid phenethyl ester-mortalin antibody nanoparticles offer enhanced selective cytotoxicity to cancer cells, Cancers 12 (9) (2020) 2370–2390, https://doi.org/10.3390/cancers12092370.

[31] D. Wang, D.B. Xiang, Y.J. He, Z.P. Li, X.H. Wu, J.H. Mou, Q.H. Zhang, Effect of caffeic acid phenethyl ester on proliferation and apoptosis of colorectal cancer cells in vitro, World J. Gastroenterol.: WJG 11 (26) (2005) 4008–4012, https://doi.org/10.3748/wjg.v11.i26.4008.

[32] M. Ersoz, A. Erdemir, D. Duranoglu, D. Uzunoglu, T. Arasoglu, S. Derman, B. Mansuroglu, Comparative evaluation of hesperetin loaded nanoparticles for anticancer activity against C6 glioma cancer cells, Artif. Cells, Nanomed., Biotechnol. 47 (1) (2019) 319–329, https://doi.org/10.1080/21691401.2018.1556213.

[33] M. Ersoz, A. Erdemir, S. Derman, T. Arasoglu, B. Mansuroglu, Quercetin-loaded nanoparticles enhance cytotoxicity and antioxidant activity on C6 glioma cells, Pharm. Dev. Technol. 25 (6) (2020) 757–766, https://doi.org/10.1080/10837450.2020.1740933.

[34] S. Goldar, M.S. Khaniani, S.M. Derakhshan, B. Baradaran, Molecular mechanisms of apoptosis and roles in cancer development and treatment, Asian Pac. J. Cancer Prev. 16 (6) (2015) 2129–2144, https://doi.org/10.7314/APJCP.2015.16.6.2129.

[35] D.T. Loo, In situ detection of apoptosis by the TUNEL assay: an overview of techniques. DNA Damage Detection In Situ, Ex Vivo, and In Vivo, Methods Protoc. (2011) 3–13, https://doi.org/10.1007/978-1-60327-409-8_1.

[36] H. Fasehee, G. Zarrinrad, S.M. Tavangar, S.H. Ghaffari, S. Faghihi, The inhibitory effect of disulfiram encapsulated PLGA NPs on tumor growth: Different administration routes, Mater. Sci. Eng.: C. 63 (2016) 587–595, https://doi.org/10.1016/j.msec.2016.03.023.

[37] V. Vijayan, K. Shalini, V. Yugesvaran, T.H. Yee, S. Balakrishnan, V.R. Palanimuthu, Effect of paclitaxel-loaded PLGA nanoparticles on MDA-MB type cell lines: apoptosis and cytotoxicity studies, Curr. Pharm. Des. 24 (28) (2018) 3366–3375, https://doi.org/10.2174/1381612824666180903110301.

[38] M.L. Wong, J.F. Medrano, Real-time PCR for mRNA quantitation, Biotechniques 39 (1) (2005) 75–85, https://doi.org/10.2144/05391RV01.

[39] R. Jan, Understanding apoptosis and apoptotic pathways targeted cancer therapeutics, Adv. Pharm. Bull. 9 (2) (2019) 205–218, https://doi.org/10.15171/apb.2019.024.

[40] M. Montazeri, M. Sadeghizadeh, Y. Pilehvar-Soltanahmadi, F. Zarghami, S. Khodi, M. Mohaghegh, N. Zarghami, Dendrosomal curcumin nanoformulation modulate apoptosis-related genes and protein expression in hepatocarcinoma cell lines, Int. J. Pharm. 509 (1–2) (2016) 244–254, https://doi.org/10.1016/j.ijpharm.2016.05.039.

[41] A.M. Abou-El-Naga, G. Mutawa, I.M. El-Sherbiny, S.A. Mousa, Activation of polymeric nanoparticle intracellular targeting overcomes chemodrug resistance in

human primary patient breast cancer cells, Int. J. Nanomed. 17 (2022) 2555–2556, https://doi.org/10.2147/IJN.S376964.
[42] S.M. Masloub, M.H. Elmalahy, D. Sabry, W.S. Mohamed, S.H. Ahmed, Comparative evaluation of PLGA nanoparticle delivery system for 5-fluorouracil and curcumin on squamous cell carcinoma, Arch. Oral. Biol. 64 (2016) 1–10, https://doi.org/10.1016/j.archoralbio.2015.12.003.
[43] A. Paul, S. Das, J. Das, A. Samadder, A.R. Khuda-Bukhsh, Cytotoxicity and apoptotic signalling cascade induced by chelidonine-loaded PLGA nanoparticles in HepG2 cells in vitro and bioavailability of nano-chelidonine in mice in vivo, Toxicol. Lett. 222 (1) (2013) 10–22, https://doi.org/10.1016/j.toxlet.2013.07.006.
[44] P. Li, L. Zhou, T. Zhao, X. Liu, P. Zhang, Y. Liu, Q. Li, Caspase-9: structure, mechanisms and clinical application, Oncotarget 8 (14) (2017) 23996–24008, https://doi.org/10.18632/oncotarget.15098.
[45] R. Mata, J.R. Nakkala, S.R. Sadras, Polyphenol stabilized colloidal gold nanoparticles from Abutilon indicum leaf extract induce apoptosis in HT-29 colon cancer cells, Colloids Surf. B: Biointerfaces 143 (2016) 499–510, https://doi.org/10.1016/j.colsurfb.2016.03.069.
[46] P.Y. Chang, S.F. Peng, C.Y. Lee, C.C. Lu, S.C. Tsai, T.M. Shieh, J.S. Yang, Curcumin-loaded nanoparticles induce apoptotic cell death through regulation of the function of MDR1 and reactive oxygen species in cisplatin-resistant CAR human oral cancer cells, Int. J. Oncol. 43 (4) (2013) 1141–1150, https://doi.org/10.3892/ijo.2013.2050.